Journal of Geodesy (1998) 72: 411–420

Journal of Geodesy

On some problems of the downward continuation of the $5' \times 5'$ mean Helmert gravity disturbance

W. Sun*, P. Vaníček

Department of Geodesy and Geomatics Engineering, University of New Brunswick, Fredericton, N.B., Canada E3B 5A3

Received: 19 August 1996 / Accepted: 4 February 1998

Abstract. This research deals with some theoretical and numerical problems of the downward continuation of mean Helmert gravity disturbances. We prove that the downward continuation of the disturbing potential is much smoother, as well as two orders of magnitude smaller than that of the gravity anomaly, and we give the expression in spectral form for calculating the disturbing potential term. Numerical results show that for calculating truncation errors the first 180° of a global potential model suffice. We also discuss the theoretical convergence problem of the iterative scheme. We prove that the $5' \times 5'$ mean iterative scheme is convergent and the convergence speed depends on the topographic height; for Canada, to achieve an accuracy of 0.01 mGal, at most 80 iterations are needed. The comparison of the "mean" and "point" schemes shows that the mean scheme should give a more reasonable and reliable solution, while the point scheme brings a large error to the solution.

Key words. Downward continuation · Helmert's gravity · Poisson integral · Disturbing potential · Gravity disturbance · Gravity anomaly

1 Introduction

The so-called downward continuation is usually defined as a reduction of gravity values from the earth surface to the geoid. It may be applied to observed gravity values, gravity disturbances, disturbing potential or any combination of these quantities.

Correspondence to: W. Sun*

*Now at: Department of Geodesy and Photogrammetry, Royal Institute of Technology, S-100 44 Stockholm, Sweden Tel: +46 8 790 7333; Fax: + 46 8 790 7343; e-mail: Sunw@geomatics.kth.se

Since the space between the earth surface and the geoid contains topographical masses with an irregular density distribution, the disturbing potential or gravity values cannot be easily reduced because they are not harmonic in this space. To overcome this difficulty, one usually transforms the real space into a model space, such as the free-air model or the Helmert model. The former is employed in the context of solving the Molodenskij problem (Moritz 1980); one simply declares the topographical masses to have a zero density while leaving the gravity anomalies on the surface intact. This results in all the high-frequency components being present in the anomalies while the masses causing the existence of these components are gone. We are interested in the Helmert model since it seems physically reasonable to determine the geoid undulation. The Helmert model uses Helmert's condensation of topography onto the geoid by means of one of the condensation techniques, that may preserve either the total mass of the earth, or the location of the centre of mass, or to be just an integral mean of topographical column density (Wichiencharoen 1982; Vaníček and Martinec 1994; Martinec and Vaníček 1994). Helmert's disturbing potential at the earth surface is thus made smoother than the actual disturbing potential because the nearest "disturbing masses" are now located on the geoid.

For the Helmert model, the basic definition of the downward continuation of Helmert gravity disturbance, denoted by $D\delta g^h$, is (Vaníček and Martinec, 1994):

$$D\delta g^h(r,\Omega,R) = \delta g_g^h(R,\Omega) - \delta g_t^h(r,\Omega) \tag{1}$$

where

$$\delta g_g^h(R,\Omega) = -\left.\frac{\partial T^h(R,\Omega)}{\partial r}\right|_g \tag{2}$$

$$\delta g_t^h(r,\Omega) = -\left.\frac{\partial T^h(r,\Omega)}{\partial r}\right|_t \tag{3}$$

T^h is Helmert's disturbing potential, R is the mean radius of the earth, r is the radial distance from the centre of the earth, Ω stands for a geocentric direction given by

latitude ϕ and longitude λ, $|_g$ and $|_t$ denote that the derivatives of T^h are taken on the geoid and the topography, respectively. The relation of the derivatives can be expressed by the Poisson integral (Heiskanen and Moritz 1967)

$$r\frac{\partial T^h(r,\Omega)}{\partial r}\bigg|_t = \frac{R}{4\pi}\int_{\Omega'}\frac{\partial T^h(R,\Omega')}{\partial r}\bigg|_g K(r,\psi,R)\,\mathrm{d}\Omega' \tag{4}$$

where K is the Poisson kernel

$$\begin{aligned} K(r,\psi,R) &= \sum_{j=2}^{\infty}(2j+1)\left(\frac{R}{r}\right)^{j+1}P_j(\cos\psi) \\ &= R\left[\frac{r^2-R^2}{(R^2+r^2-2Rr\cos\psi)^{\frac{3}{2}}}-\frac{1}{r}-\frac{3R}{r^2}\cos\psi\right] \end{aligned} \tag{5}$$

and ψ is the angular distance between geocentric directions Ω and Ω', and $P_j(\cos\psi)$ is the Legendre polynomial of degree j.

Then from the fundamental equation of physical geodesy (Heiskanen and Moritz 1967, p.86)

$$\Delta g_g = -\frac{\partial T}{\partial r}\bigg|_g - \frac{2}{R}T_g \tag{6}$$

which is valid even for the Helmert model, we can obtain the expression for $D\delta g^h$ as

$$D\delta g^h(r,\Omega,R) = D\Delta g^h(r,\Omega,R) + DT^h(r,\Omega,R) \tag{7}$$

where

$$\begin{aligned} &D\Delta g^h(r,\Omega,R) \\ &\quad = \Delta g_g^h(\Omega) - \frac{R}{4\pi r}\int_{\Omega'}\Delta g_g^h(\Omega')K(r,\psi,R)\;\mathrm{d}\Omega' \end{aligned} \tag{8}$$

$$\begin{aligned} &DT^h(r,\Omega,R) \\ &\quad = \frac{2}{R}T_g^h(\Omega) - \frac{1}{2\pi r}\int_{\Omega'}T_g^h(\Omega')K(r,\psi,R)\;\mathrm{d}\Omega' \end{aligned} \tag{9}$$

are called the downward continuation of Helmert's gravity anomaly and the downward continuation of Helmert's disturbing potential $2T^h/R$.

The second term on the right-hand side of Eq. (8) is nothing but the Helmert gravity anomaly on the topography, i.e.

$$\Delta g_t^h(\Omega) = \frac{R}{4\pi r}\int_{\Omega'}\Delta g_g^h(\Omega')K(r,\psi,R)\;\mathrm{d}\Omega' \tag{10}$$

which can be easily derived from the Poisson integrals for T^h and $\partial T^h/\partial r$ and the fundamental Eq. (6) by changing the subscript g to t. Now the problem of the downward continuation is to determine $D\Delta g^h(r,\Omega,R)$ and $DT^h(r,\Omega,R)$ on the geoid from the known Helmert gravity anomaly $\Delta g_t^h(\Omega)$ and a global model of the disturbing potential $T_t(\Omega)$. Once $D\Delta g^h(r,\Omega,R)$ and $DT^h(r,\Omega,R)$ are known, the downward continuation of the Helmert gravity disturbance can be simply obtained from Eq. (7).

Vaníček et al. (1996) have studied the downward continuation of the $5'\times 5'$ mean Helmert gravity anomaly. They divided the gravity anomalies into two parts: low frequency and high frequency. The former was calculated from the satellite-determined potential coefficients and the latter was obtained from the observed gravity on the earth surface. They truncated the Poisson integration and modified the Poisson kernel to reduce the truncation error. They proposed an iterative scheme to perform the downward continuation to obtain the Helmert gravity anomalies. They claimed that the determination of the downward continuation of the mean $5'\times 5'$ Helmert gravity anomalies is a well-posed problem with a unique solution and can be carried out routinely to any accuracy desired in the geoid computation. This proves that a discretized system of (Poisson) integral equations can always be solved (Bjerhammar 1963, 1964, 1987) for the $5'\times 5'$ discretization.

In this paper, we are going to investigate some theoretical and numerical problems of the downward continuation of the $5'\times 5'$ mean Helmert gravity disturbances by taking the disturbing potential into account. This research will answer the following questions: how to calculate the downward continuation of the disturbing potential term conveniently; how many degrees of a global potential model should be considered for calculating the truncation error; how fast does the iterative scheme converge; and which scheme is better, that based on block mean value or that based on point value.

2 Downward continuation of the potential term

In this section we discuss how to calculate the downward continuation term of the potential DT^h in Eq. (9). First, we prove the conclusion given in Vaníček et al. (1996), i.e. for the degree n of the model equal to 180, the value of T^h drops by two orders of magnitude compared to Δg^h. Then we discuss how to calculate the downward continuation of this term and give the expressions in spectral form.

The disturbing potential and gravity anomaly on the geoid can be expanded into spherical harmonics as

$$T(\Omega) = \sum_{j=2}^{\infty}\sum_{m=-j}^{j}[T]^{jm}(\Omega) \tag{11}$$

$$\Delta g(\Omega) = \sum_{j=2}^{\infty}(j-1)\sum_{m=-j}^{j}[\Delta g]^{jm}(\Omega) \tag{12}$$

where $[T]^{jm}(\Omega)$ and $[\Delta g]^{jm}(\Omega)$ are the harmonic components of $T(\Omega)$ and $\Delta g(\Omega)$, respectively

$$\forall jm:\ [T]^{jm}(\Omega) = \frac{GM}{R}T_{jm}Y_{jm}(\Omega) \tag{13}$$

$$\forall jm:\ [\Delta g]^{jm}(\Omega) = \frac{GM}{R^2}(j-1)T_{jm}Y_{jm}(\Omega) \tag{14}$$

Then, for each harmonic component, we have

$$\forall jm:\ \frac{2}{R}[T]^{jm}(\Omega) : [\Delta g]^{jm}(\Omega) = 2:(j-1) \tag{15}$$

This indicates that while for low degrees (say, $j<10$), $\frac{2}{R}[T]^{jm}(\Omega)$ and $[\Delta g]^{jm}(\Omega)$ are of the same order, i.e. they

give the same contribution to the result $D\delta g$, for high degrees, the latter becomes larger than the former.

On the other hand, if we solve the Poisson integral in a local area by truncating it at $\psi_0 = 1^\circ$ because of the fact that the Poisson kernel drops very fast and the most power distribution is within 1° (Vaníček et al. 1996), the local contribution to the downward continuation of anomalous gravity only comes from about $j > 180$. In this case, we know from Eq. (15) that the contribution from the disturbing potential $\frac{2}{R}[T]^{jm}(\Omega)$ is two orders of magnitude smaller than that from the gravity anomaly part $[\Delta g]^{jm}(\Omega)$.

We therefore conclude that the disturbing potential part $\frac{2}{R}T_g^h(\Omega)$ is much smoother and smaller than the gravity part $\Delta g_g^h(\Omega)$. We thus assume that Eq. (7) can be simplified as

$$D\delta g^h(r,\Omega,R) = D\Delta g^h(r,\Omega,R) + DT(r,\Omega,R) \tag{16}$$

and that the downward continuation of $\frac{2}{R}T^h$ can be numerically estimated from a global potential model, neglecting the Helmert condensation operation, i.e. as

$$DT(r,\Omega,R) = \frac{2}{R}T_g(\Omega) - \frac{1}{2\pi r}\int_{\Omega'} T_g(\Omega')K(r,\psi,R)\ \mathrm{d}\Omega' \tag{17}$$

To calculate $DT(r,\Omega,R)$ we have to transform Eq. (17) into a spectral form because the global disturbing potential model T is usually given in a spectral form. Substituting the spectral form of potential $T_g(\Omega)$ and Poisson kernel $K(r,\psi,R)$ in Eq. (5) into the second term on the right-hand side of Eq. (17), we have

$$\begin{aligned}\frac{1}{2\pi r}\int_{\Omega'} T_g(\Omega')K(r,\psi,R)\ \mathrm{d}\Omega' &= \frac{1}{2\pi r}\int_{\Omega'}\frac{GM}{R}\sum_{j_1=2}^{\infty}\sum_{m_1=-j_1}^{j_1} T_{j_1m_1}Y_{j_1m_1}(\Omega') \\ &\quad\times\sum_{j=2}^{\infty}(2j+1)\left(\frac{R}{r}\right)^{j+1}P_j(\cos\psi)\ \mathrm{d}\Omega'\end{aligned} \tag{18}$$

Considering the following formulae

$$\frac{4\pi}{2j+1}\sum_{m=-j}^{j} Y_{jm}^*(\Omega')Y_{jm}(\Omega) = P_j(\cos\psi) \tag{19}$$

$$\int_{\Omega} Y_{j_1m_1}^*(\Omega)Y_{j_2m_2}(\Omega)\ \mathrm{d}\Omega = \delta_{j_1j_2}\delta_{m_1m_2} \tag{20}$$

Eq. (18) becomes

$$\begin{aligned}\frac{1}{2\pi r}\int_{\Omega'} T_g(\Omega')K(r,\psi,R)\ \mathrm{d}\Omega' &= \frac{R\gamma}{r}\sum_{j=2}^{\infty}2\left(\frac{R}{r}\right)^{j+1} \\ &\quad\times\sum_{m=-j}^{j} T_{jm}Y_{jm}(\Omega)\end{aligned} \tag{21}$$

Finally we obtain the spectral form of the downward continuation of $2T/R$ by adding to Eq. (21) the first term on the right-hand side of Eq. (17) as

$$\begin{aligned}DT(r,\Omega,R) &= 2\gamma\sum_{j=2}^{\infty}\sum_{m=-j}^{j} T_{jm}Y_{jm}(\Omega) \\ &\quad -\frac{R\gamma}{r}\sum_{j=2}^{\infty}2\left(\frac{R}{r}\right)^{j+1}\sum_{m=-j}^{j} T_{jm}Y_{jm}(\Omega) \\ &= 2\gamma\sum_{j=2}^{\infty}\left[1-\left(\frac{R}{r}\right)^{j+2}\right]\sum_{m=-j}^{j} T_{jm}Y_{jm}(\Omega) \\ &\doteq \frac{2H\gamma}{R}\sum_{j=2}^{\infty}(j+2)\sum_{m=-j}^{j} T_{jm}Y_{jm}(\Omega)\end{aligned} \tag{22}$$

where H is the topographic height.

3 Truncated integration

In our first paper (Vaníček et al. 1996), following the Molodenskij technique (Molodenskij et al. 1962; Vaníček and Sjöberg 1991), we derived the truncation error of the truncated Poisson integration in spectral form to be

$$Dg_T(\Omega) = \frac{R\gamma}{2r}\sum_{j=2}^{\infty}(j-1)\overline{Q}_j(H,\psi_0)\sum_{m=-j}^{j} T_{jm}Y_{jm}(\Omega) \tag{23}$$

where $\overline{Q}_j(H,\psi_0)$ are the so-called Molodenskij coefficients.

It is natural to study the summation in Eq. (23) at some degree. To what degree the limited summation can give results with sufficient accuracy is a question to be answered. In the following we arrive at the answer through numerical calculations.

Since we have chosen $\psi_0 = 1^\circ$ as the truncation angle (Vaníček et al. 1996), the contribution to the truncation error should come mostly from the first 180° of the global potential model. Also, most of the power of a global potential model, e.g. GFZ93a, (Gruber and Anzenhofer 1993) in Fig. 1, is at the first 50° and becomes almost constant after degree 180. We calculated the truncation error with degree n for two typical points, plotted in Fig. 2. The results indicate that the first 50° give results good to 0.02 mGal. Above degree 180 the truncation error estimate reaches an accuracy of 0.01 mGal. Hence we only need to consider the first 180° of a global potential model for calculating the truncation error.

Since satellite gravimetry provides a low-frequency potential model with very high accuracy, we split the gravity anomaly (on both the topography and the geoid) into two parts: low-frequency part $(\Delta g^h)_L$ and high-frequency part $(\Delta g^h)^L$ (see the Appendix in Vaníček et al. 1996). The low-frequency part of gravity anomaly is calculated from a global potential model. We focus our study here on the high-frequency part: once we obtain the high-frequency part of gravity anomaly $(\Delta g_g^h)^L$ we can get the whole gravity anomaly Δg_g^h by adding to it the low-frequency part $(\Delta g_g^h)_L$.

To obtain $(\Delta g_g^h)^L$, the integration in Eq. (10) can be truncated to a spherical cap C_0 so that

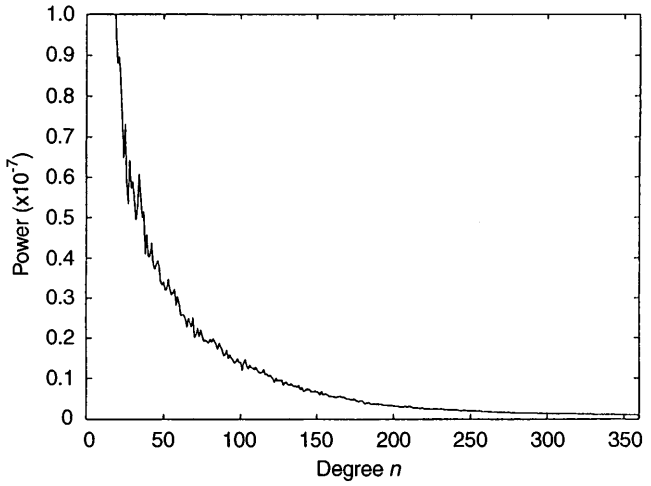

Fig. 1. Power $\left[\sum_{m=-n}^{n}(C_{nm}^2+S_{nm}^2)\right]^{1/2}$ (where C_{nm} and S_{nm} are the harmonic coefficients of the global potential model GFZ93a) for individual degrees n

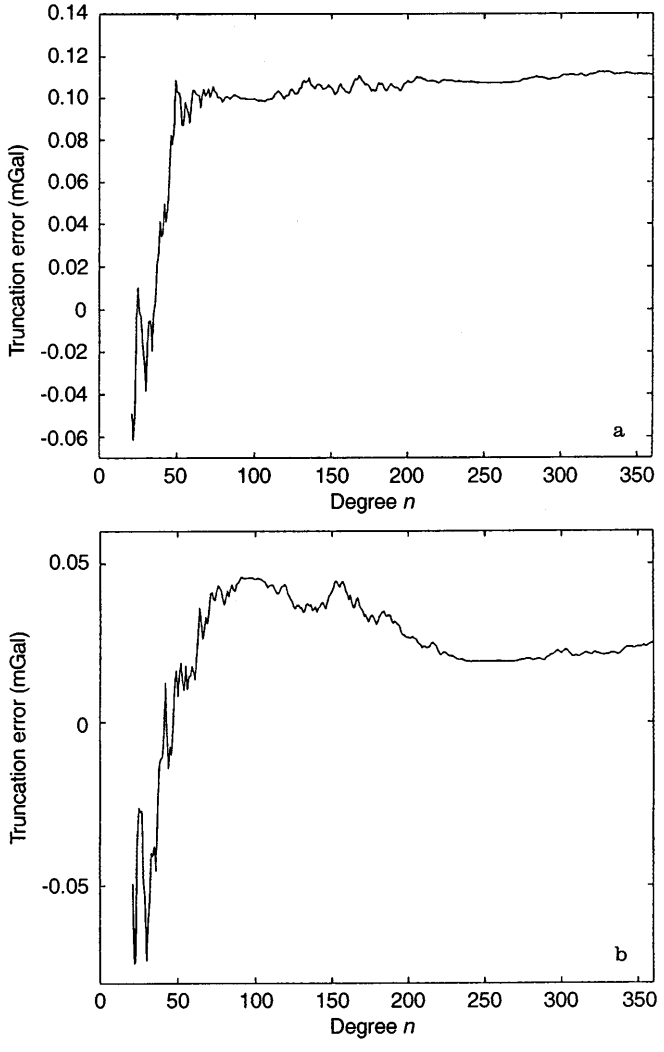

Fig. 2a, b. Estimates of truncation errors (mGal) of 1° truncated integration for two points: **a** point of (38.71°, 241.5°, 2 km) and **b** point of (38.96°, 244.5°, 2 km), plotted as function of n

$$(\Delta g_t^h)^L = \frac{R}{4\pi r}\int_{C_0}(\Delta g_g^h)^L K^m(H,\psi,\psi_0)\,\mathrm{d}\Omega' \;+\; Dg_T \qquad (24)$$

where ψ_0 is the radius of C_0 (truncation angle), Dg_T is the truncation error (Eq. 23) and

$$K^m(H,\psi,\psi_0) = K(H,\psi) - \sum_{j=0}^{L}\frac{2j+1}{2}t_j(H,\psi_0)P_j(\cos\psi) \qquad (25)$$

is the modified Poisson kernel with unknown coefficients t_j, which can be determined for a given H and ψ_0 (see Table 1) that the upper limit of the truncation error is minimized.

The integration of the first term of Eq. (24) over the 1° spherical cap must in practice be done numerically by summing over geographical cells of specified dimensions. It is thus reasonable to use the same mean anomalies on the same geographical grid as in Stokes's integration. In Canada we use $5' \times 5'$ cells after Vaníček and Kleusberg (1987). Then from Eq. (24) we may obtain the mean anomaly in the i-th cell in the grid as

$$\overline{(\Delta g_t^h)_i^L} = \frac{R}{4\pi r}\sum_j \overline{(\Delta g_g^h)^L}_j\,\overline{\overline{K_{ij}^m}} + \overline{Dg_T}_i \qquad (26)$$

where

$$\overline{\overline{K_{ij}^m}} = \frac{1}{A_i}\int_{c_i}\int_{c_j} K^m[H(\Omega_i),\Omega_i,\Omega']\,\mathrm{d}\Omega'\,\mathrm{d}\Omega \qquad (27)$$

is the doubly averaged (integrated) modified Poisson kernel for the i-th and j-th cells and the summation is taken over all the cells contained within the integration cap of radius ψ_0, and A_i is the area of the i-th cell.

4 Convergence speed of the $5' \times 5'$ iterative scheme

Equation (26) can be solved by setting up the iterative scheme (Vaníček et al. 1996), expressed in the vector-matrix form as

$$\overline{\mathbf{q}}^{(n+1)} = \overline{\mathbf{q}}^{(n)} - \mathbf{B}\overline{\mathbf{q}}^{(n)} \qquad (28)$$

where the initial value $\overline{\mathbf{q}}^{(0)}$ is the difference of the high-frequency part of the mean Helmert gravity anomaly on the topography $\overline{\Delta \mathbf{g}_t^h}$ and the truncation error $\overline{\mathbf{Dg}_T}$

$$\overline{\mathbf{q}}^{(0)} = \overline{(\Delta \mathbf{g}_t^h)^L} - \overline{\mathbf{Dg}_T} \qquad (29)$$

The coefficient matrix $\mathbf{B}$ has a simple relation with the integrated modified Poisson kernel $\overline{\overline{\mathbf{K}^m}}$:

$$\mathbf{B} = \frac{R}{4\pi r}\overline{\overline{\mathbf{K}^m}} \qquad (30)$$

Equation (28) can be easily reformulated as a multiplication of a matrix and the initial vector $\overline{\mathbf{q}}^{(0)}$, i.e.

$$\overline{\mathbf{q}}^{(n)} = (\mathbf{I}-\mathbf{B})^n\overline{\mathbf{q}}^{(0)} \qquad (31)$$

Table 1 Coefficients t_j for some heights ($\psi_0 = 1°$)

j	$H = 100$ m	$H = 500$ m	$H = 1000$ m	$H = 2000$ m	$H = 3000$ m	$H = 4500$ m
0	−0.19981E+01	−0.19907E+01	−0.19814E+01	−0.19628E+01	−0.19442E+01	−0.19163E+01
1	−0.19981E+01	−0.19907E+01	−0.19814E+01	−0.19628E+01	−0.19442E+01	−0.19163E+01
2	0.17688E−02	0.88436E−02	0.17685E−01	0.35360E−01	0.53021E−01	0.79475E−01
3	0.17383E−02	0.86907E−02	0.17379E−01	0.34749E−01	0.52104E−01	0.78100E−01
4	0.17080E−02	0.85391E−02	0.17076E−01	0.34143E−01	0.51195E−01	0.76737E−01
5	0.16779E−02	0.83889E−02	0.16776E−01	0.33542E−01	0.50294E−01	0.75386E−01
6	0.16481E−02	0.82401E−02	0.16478E−01	0.32947E−01	0.49402E−01	0.74048E−01
7	0.16186E−02	0.80926E−02	0.16183E−01	0.32357E−01	0.48517E−01	0.72721E−01
8	0.15894E−02	0.79465E−02	0.15891E−01	0.31773E−01	0.47641E−01	0.71407E−01
9	0.15604E−02	0.78017E−02	0.15602E−01	0.31194E−01	0.46772E−01	0.70105E−01
10	0.15318E−02	0.76582E−02	0.15315E−01	0.30620E−01	0.45912E−01	0.68815E−01
11	0.15033E−02	0.75161E−02	0.15030E−01	0.30052E−01	0.45060E−01	0.67537E−01
12	0.14752E−02	0.73754E−02	0.14749E−01	0.29489E−01	0.44216E−01	0.66271E−01
13	0.14473E−02	0.72359E−02	0.14470E−01	0.28932E−01	0.43380E−01	0.65018E−01
14	0.14197E−02	0.70979E−02	0.14194E−01	0.28379E−01	0.42552E−01	0.63776E−01
15	0.13923E−02	0.69611E−02	0.13921E−01	0.27833E−01	0.41732E−01	0.62547E−01
16	0.13652E−02	0.68257E−02	0.13650E−01	0.27291E−01	0.40920E−01	0.61329E−01
17	0.13384E−02	0.66917E−02	0.13382E−01	0.26755E−01	0.40116E−01	0.60124E−01
18	0.13119E−02	0.65590E−02	0.13116E−01	0.26224E−01	0.39320E−01	0.58931E−01
19	0.12856E−02	0.64276E−02	0.12854E−01	0.25699E−01	0.38532E−01	0.57749E−01
20	0.12596E−02	0.62975E−02	0.12594E−01	0.25179E−01	0.37752E−01	0.56580E−01

where $\mathbf{I}$ is the unit matrix. Then the mean Helmert gravity anomaly on the geoid has the following form

$$\overline{(\Delta \mathbf{g}_g^h)^L} = \left[\sum_{n=0}^{\infty} (\mathbf{I} - \mathbf{B})^n\right] \overline{\mathbf{q}}^{(0)} \tag{32}$$

and the downward continuation of mean Helmert gravity disturbance (Eq. 7) can be rewritten as

$$\overline{(\mathbf{D}\delta \mathbf{g}^h)^L} \doteq -\left[\sum_{n=1}^{N} (\mathbf{I} - \mathbf{B})^n\right] \overline{\mathbf{q}}^{(0)} - \overline{\mathbf{DT}} \tag{33}$$

The questions to be answered are whether or not the given iterative scheme converges [i.e. can we take a finite integer N in Eq. (33)] and if it does then how fast and how to determine the number N?

First, we infer from Eqs. (31) and (32) that if the norm of an individual iteration $\overline{\mathbf{q}}^{(n)}$ becomes smaller and smaller as n increases, the iteration must converge in that norm. Equation (31) indicates that whether or not $\overline{\mathbf{q}}^{(n)}$ becomes smaller with n depends on the following condition

$$\lim_{n\to\infty} (\mathbf{I} - \mathbf{B})^n = \mathbf{0} \tag{34}$$

because the initial vector $\overline{\mathbf{q}}^{(0)}$ is constant. Since for any H the elements of $\mathbf{B}$ based on the doubly averaged Poisson kernel take values between 0 and 1, then $\left|(\mathbf{I} - \mathbf{B})_{ij}\right| < 1 \ \forall i, j$, therefore the condition given by Eq. (34) must be satisfied. This proves that the foregoing iterative scheme converges.

Next, let us discuss the speed of convergence. We can see from Eq. (34) that the speed of convergence depends on the B_{ij} values: the larger the diagonal values B_{ii}, the smaller the off-diagonal values B_{ij} (because the sum of the diagonal and off-diagonal values in each row is fixed – see the next section for details) and the faster the convergence. A closer look at $\mathbf{B}$ shows that $\mathbf{B}$ varies mainly with height and slightly with latitude [since the cell size is $(5' \times 5') \sin\theta$]. For any height the largest value appears at the diagonal. Figure 3 gives a plot of the diagonal values of $\mathbf{B}$ at the latitude of 72°N. It shows that the larger the height, the smaller the B_{ii} value. This means that the convergence speed for larger height should be slower than for smaller height.

In the following we investigate the convergence speed in detail. Figure 4 shows the decrease in $|[1 - B_{ii}(H)]^n|$ with n for four heights (100, 1000, 3000 and 4500 m) at a latitude of 72°N.

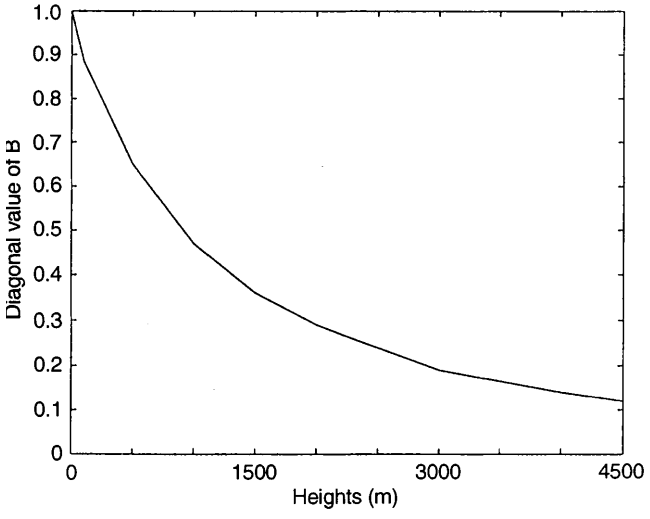

Fig. 3. Diagonal values of $\mathbf{B}$ for different heights and latitude 72°

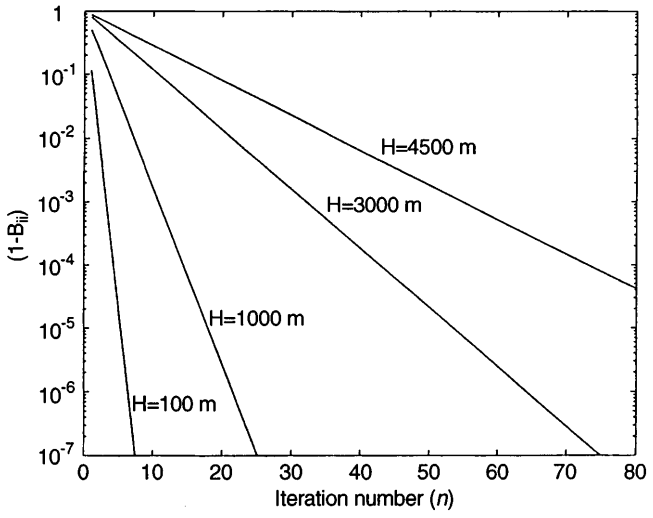

Fig. 4. Convergence of $[1 - B_{ii}(H_i)]^n$ with n

We can see that $|[1 - B_{ii}(H)]^n|$ has rather different values for different heights. In the case of $H = 100$ m, $|[1 - B_{ii}(H)]^n|$ drops to about 10^{-3} at $n = 4$, while in the case of $H = 4500$ m, $|[1 - B_{ii}(H)]^n|$ decreases to 10^{-3} at about $n = 64$. Usually, the initial value $\overline{q}_i^{(0)}$ is at most a few hundreds of mGals. For example, $\max_i \left|\overline{q}_i^{(0)}\right|$ in the Canadian Rocky Mountains (delimited by latitudes 41° N and 62°N, and longitudes 223°E and 259°E) is 205 mGal. In this area, the maximum mean height for $5' \times 5'$ is 3612 m and for this cell $\overline{q}_i^{(0)} = 152$ mGal. We know from Eq. (31) that $|\overline{q}_i|$ becomes less than 0.01 mGal when $|[1 - B_{ii}(H)]^n|$ drops to 0.658×10^{-4}. [This is what we require to get a centimetre geoid (Vaníček and Martinec 1994)]. Figure 4 shows that 0.658×10^{-4} corresponds to an n between 40 and 50. Since the highest mean height in Canada is less than 4500 m, we may learn from Fig. 4 (taking $\overline{q}_i^{(0)} = 152$ mGal) that at most 80 iterations are enough for Canada.

Let $W = \ln(1 - B_{ii}(H))^n$ be the convergence speed; we can obtain from Fig. 4 an empirical formula

$$W = -\frac{3n}{H} \tag{35}$$

where H is the topographical height in km. Equation (35) shows that the convergence speed is directly proportional to n and inversely proportional to H. On the other hand, when W is fixed (to reach at an accuracy requirement), then n and H have a linear proportional relation.

We have to point out that the foregoing discussion is a pessimistic convergence estimate because we only considered the diagonal terms. As the geographical cells become smaller (smaller than $5' \times 5'$), the off-diagonal contributions will become larger. Even for the $5' \times 5'$ scheme the off-diagonal terms may have some effect on the convergence speed even though they are not too large. However, both the foregoing discussion and Martinec (1996) have shown that the $5' \times 5'$ scheme is convergent.

5 Comparison of the "mean" and "point" schemes

To evaluate the downward continuation in practice, one has to discretize the Poisson integral of Eq.(10) into a system of linear equations. There are two ways to carry this out. One way is to use mean values as already shown (Vaníček et al. 1996). The discrete Poisson integral gives the following system of linear equations

$$\overline{\Delta \mathbf{g}_\mathbf{t}^\mathbf{h}} = \mathbf{B}\overline{\Delta \mathbf{g}_\mathbf{g}^\mathbf{h}} \tag{36}$$

where the matrix coefficients B_{ij} are defined (Eqs. 27 and 30) as

$$\forall ij, H: \; B_{ij} = \frac{R}{4\pi r A_i} \int_{c_i} \int_{c_j} K^m(H(\Omega), \Omega, \Omega')\, \mathrm{d}\Omega'\, \mathrm{d}\Omega \tag{37}$$

Actually this scheme uses integral means in cells, evaluated from the Mean Value Theorem.

The other way was used by Martinec (1996), in which the Poisson integral is simply discretized by using the value of the Poisson kernel at the central point of each cell. His results are on average about five times smaller than those obtained from the mean scheme. This represents a numerical quadrature of the crudest kind. The corresponding system of linear equations is

$$\Delta \mathbf{g}_\mathbf{t}^\mathbf{h} = \mathbf{C}\Delta \mathbf{g}_\mathbf{g}^\mathbf{h} \tag{38}$$

where $\mathbf{C}$ is the matrix composed of

$$\forall ij, H: \; C_{ij} = \frac{R}{4\pi r} K^m(H(\Omega), \Omega, \Omega') A_j \tag{39}$$

where A_j is the area of the j-th cell.

In the following we compare the two schemes to see what differences exist between them, where the factor 5 (of the difference between the point and mean schemes) comes from, and which scheme is more reasonable. We first investigate the behaviour of the modified Poisson kernel K^m given in Eq. (25), which can be rewritten as

$$K^m(H, \psi, \psi_0) = \left[\sum_{j=2}^{\infty} (2j+1)\left(\frac{R}{r}\right)^{j+1} - \sum_{j=0}^{L} \frac{2j+1}{2} t_j(H, \psi_0)\right] P_j(\cos\psi) \tag{40}$$

Integrating K^m over a unit sphere gives

$$\begin{aligned} &\int_\Omega K^m(H, \psi, \psi_0)\, \mathrm{d}\Omega \\ &\quad = \left[\sum_{j=2}^{\infty} (2j+1)\left(\frac{R}{r}\right)^{j+1} - \sum_{j=0}^{L} \frac{2j+1}{2} t_j(H, \psi_0)\right] \\ &\qquad \times \int_\Omega P_j(\cos\psi)\, \mathrm{d}\Omega \\ &\quad = \left[\sum_{j=2}^{\infty} (2j+1)\left(\frac{R}{r}\right)^{j+1} - \sum_{j=0}^{L} \frac{2j+1}{2} t_j(H, \psi_0)\right] \cdot 4\pi\delta_{j0} \\ &\quad = -2\pi t_0(H, \psi_0) \end{aligned} \tag{41}$$

where the following property of Legendre's functions is used

$$\forall j: \quad \int_{\Omega} P_j(\cos\psi)\,\mathrm{d}\Omega = 4\pi\delta_{j0} \tag{42}$$

Table 1 gives

$$t_0(H, 1^\circ) = -2 + O\left(\frac{H}{R}\right) \tag{43}$$

and the integral mean of the modified Poisson kernel K_m over the unit sphere is

$$\frac{1}{4\pi}\int_{\Omega} K^m(H, \psi, \psi_0)\,\mathrm{d}\Omega = 1 - O\left(\frac{H}{R}\right) \tag{44}$$

After truncation at 1° and modification, the low-frequency part of Poisson's kernel is removed (see Vaníček et al. 1996, Figs. 3 and 4). The modified Poisson kernel K^m then has the following property

$$\frac{1}{4\pi}\int_{1^\circ}^{\pi} K^m(H, \psi, 1^\circ)\,\mathrm{d}\psi \;\approx\; 0 \tag{45}$$

This implies that Eq. (44) can be expressed as

$$\frac{1}{4\pi}\int_{\psi<1^\circ} K^m(H, \psi, 1^\circ)\,\mathrm{d}\Omega \;\approx\; 1 \tag{46}$$

i.e. the average of the modified Poisson kernel K_m over the cap of 1° is equal to about 1.

Equation (46) describes the behaviour of the modified Poisson kernel important in discussing the two discrete schemes. According to Eq. (46), the sum of the matrix coefficents B_{ij} in Eq. (37) and C_{ij} in Eq. (39) should be

$$\forall i: \quad \sum_{j}^{M} B_{ij} \doteq 1 \tag{47}$$

$$\forall i: \quad \sum_{j}^{M} C_{ij} \doteq 1 \tag{48}$$

where M is the cell number over the cap of 1°. To test this, we here calculated the two sums for different heights on latitude of 72°N. The results are plotted in Fig. 5 they show that

$$\sum_{j}^{M} B_{ij} \doteq 1 \tag{49}$$

$$\sum_{j}^{M} C_{ij} > 1 \tag{50}$$

The results also show that the lower the height, the larger the sum $\sum_j^M C_{ij}$, e.g. for $H = 100$ m, $\sum_j^M C_{ij}$ is more than two orders of magnitude larger than 1. The large difference between the two sums comes mainly from the central $5' \times 5'$ cell of the 1° cap, i.e. from the diagonal values B_{ii} and C_{ii}. Figure 6 gives the diagonal values B_{ii} and C_{ii}: it shows similar features to Fig. 5, especially for the smaller heights. This could be easily understood because the lower the height, the larger the

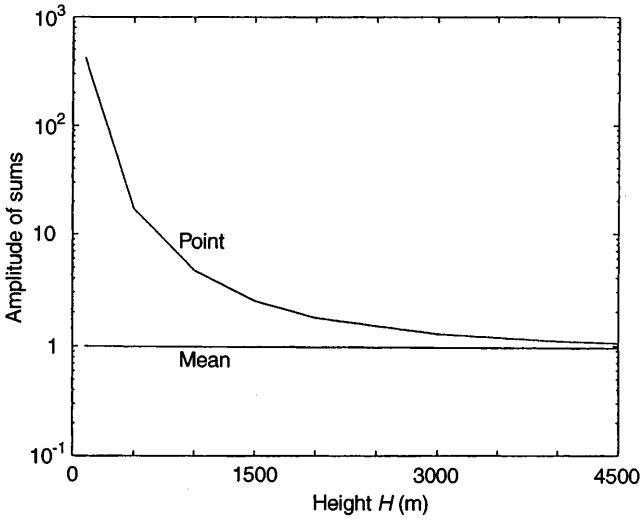

Fig. 5. Sums of matrix elements B_{ij} and C_{ij} for different heights on a cap of 1° radius for $\phi = 72^\circ$

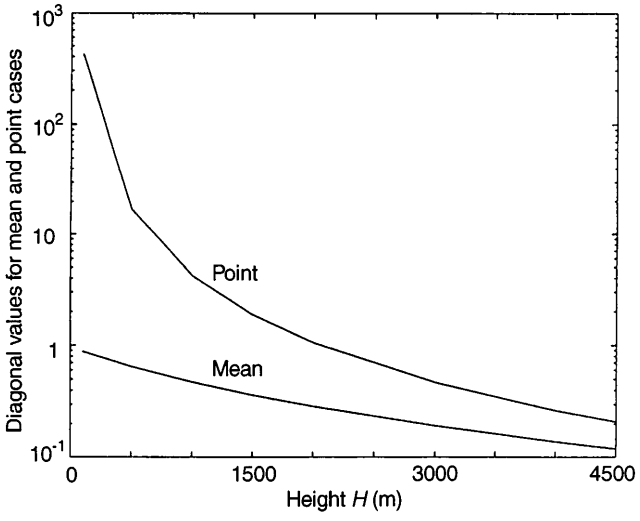

Fig. 6. Diagonal elements B_{ii} and C_{ii} of matrices **B** and **C** as function of heights for $\phi = 72^\circ$

contribution from the central cell. In particular in the case of $H = 0$, the Poisson kernel becomes a δ-function and the whole contribution of the Poisson kernel is in the central point (cell). Note that in this case the mean (integrated) value B_{ii} is still equal to 1, while the point value $C_{ii}(H = 0)$ grows to infinity.

We now rewrite Eqs. (36) and (38) in a component form

$$\forall ij: \quad \overline{\Delta g^h_{t\,i}} = \sum_{j} B_{ij}\overline{\Delta g^h_{gj}} \tag{51}$$

$$\forall ij: \quad \Delta g^h_{ti} = \sum_{j} C_{ij}\Delta g^h_{gj} \tag{52}$$

Both theoretical and numerical results show that for smaller heights the diagonal terms (B_{ii} and C_{ii}) dominate over the off-diagonal terms (B_{ij} and C_{ij}, $j \neq i$), i.e.

$$\forall i, j \neq i: \quad |B_{ii}| \gg |B_{ij}| \tag{53}$$

$$\forall i, j \neq i: \quad |C_{ii}| \gg |C_{ij}| \tag{54}$$

For small heights, to estimate the effect of **B** and **C** on the downward continuation of gravity, we may consider only the diagonal terms, so that Eqs. (51) and (52) can be simplified as

$$\forall i: \quad \overline{\Delta g^h_{t\,i}} \doteq B_{ii}\overline{\Delta g^h_{g\,i}} \tag{55}$$

$$\forall i: \quad \Delta g^h_{ti} \doteq C_{ii}\Delta g^h_{gi} \tag{56}$$

since the other elements $B_{ij}\overline{\Delta g^h_{g\,j}}$ of $\mathbf{B}_i\overline{\Delta \mathbf{g}^{\mathbf{h}}_{\mathbf{g}}}$ would be much smaller. Then the corresponding inverses are

$$\forall i: \quad \overline{\Delta g^h_{gi}} \doteq B^{-1}_{ii}\overline{\Delta g^h_{ti}} \tag{57}$$

$$\forall i: \quad \Delta g^h_{gi} \doteq C^{-1}_{ii}\Delta g^h_{ti} \tag{58}$$

Theoretically, the mean values are smaller than (in absolute value) or equal to the point values:

$$\forall i: \quad |\overline{\Delta g^h_{ti}}| \leq |\Delta g^h_{ti}| \tag{59}$$

To investigate the difference between the two schemes we shall assume that the point and mean Helmert gravity anomalies are the same, i.e.

$$\forall i: \quad \overline{\Delta g^h_{ti}} = \Delta g^h_{ti} \tag{60}$$

This assumption is reasonable in practical calculation, because in many cases we do not observe gravity at too many points in each $5' \times 5'$ cell. The difference of the point and mean gravity depends on what method is used in processing the observed gravity data and is usually small or zero. Under the assumption of Eq. (60), the relation between $\overline{\Delta g^h_g}$ and Δg^h_g depends only on the ratio Q_i, which is

$$\forall i: \quad Q_i = \frac{B^{-1}_{ii}}{C^{-1}_{ii}} = \frac{C_{ii}}{B_{ii}} \tag{61}$$

Then we have

$$\forall i: \quad \overline{\Delta g^h_{gi}} = Q_i \Delta g^h_{g\,i} \tag{62}$$

Figure 7 gives the ratio Q_i. It shows that the ratio varies from 2 ($H = 4500$ m) to several hundreds (for lower height). Since the ratio Q_i is always larger than 1, we have

$$\forall i: \quad \overline{\Delta g^h_{gi}} > \Delta g^h_{gi} \tag{63}$$

For example, for an area with the highest height of 1500 m, the ratio reaches 5. This means that Δg^h_g is about five times smaller than $\overline{\Delta g^h_g}$. This explains why Martinec's (1996) results are on average about five times smaller than ours. The preceding discussions show that the mean scheme is more reasonable and reliable, and the point scheme brings a large error to results because of its simple discretization of the Poisson integral.

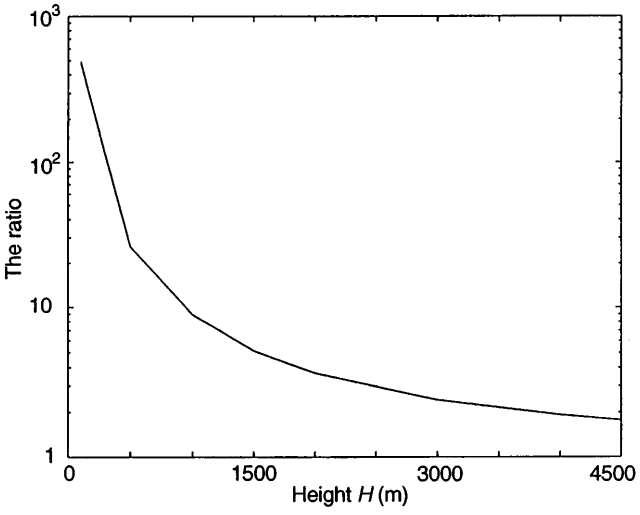

Fig. 7. The ratio Q_i

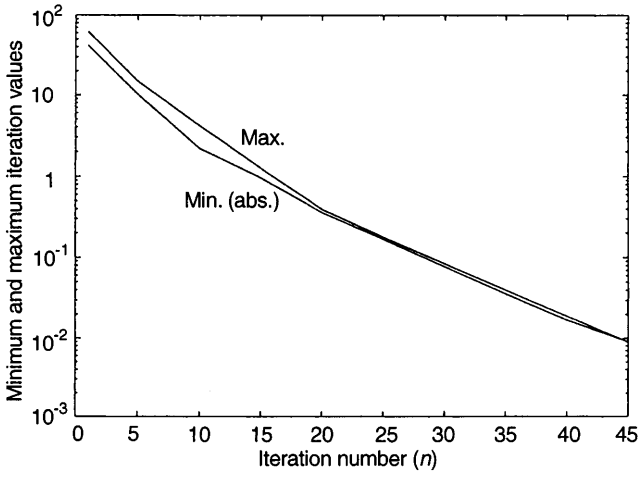

Fig. 8. Values $\overline{q}^{(n)}_{\max}$ and $\left|\overline{q}^{(n)}_{\min}\right|$ decreasing with iteration numbers n

6 Calculations and discussions

We have calculated, using an iterative technique, the downward continuation of $5' \times 5'$ mean Helmert gravity anomalies for our selected area of the Canadian Rocky Mountains delimited by latitudes 41°N and 62°N, and longitudes 223°E and 259°E (the same area as adopted in Vaníček et al., 1996). The mean $5' \times 5'$ heights in this area are between 0 and 3612 m. The mean Helmert anomalies on topography (initial vector $\overline{\mathbf{q}}^{(0)}$) have values between −131 and 205 mGal.

First, we have investigated the convergence of the iterations in the sense of Tchebyshev norm. We judge the convergence achieved when the following condition is met

$$\forall i: \quad \left|\overline{q}^{(n)}_i\right| < 0.01\,\text{mGal} \tag{64}$$

Figure 8 gives the plots of both $(\overline{q}^{(n)}_i)_{\max}$ and $\left|(\overline{q}^{(n)}_i)_{\min}\right|$ as functions of n. It indicates that $(\overline{q}^{(n)}_i)_{\max}$ and $\left|(\overline{q}^{(n)}_i)_{\min}\right|$

converge almost at the same speed and that they satisfy Eq. (64) at 45 iterations. This confirms our theoretical prediction of the number of necessary iterations being $40 < N < 50$.

The profiles of the high-frequency (higher than degree 20) part of the mean Helmert gravity anomalies on the topography and on the geoid show the same general shape but differences in amplitudes (Fig. 9); the range of the anomaly on the geoid is larger than that on the topography. The peaks of the anomaly on the geoid are always higher and the lows are lower than those of the anomaly on the topography. This makes physical sense. The mean values before and after the downward continuation over the selected area increase, i.e. the average of Δg_t^h is -2.897 mGal and the average of Δg_g^h is 0.387 mGal. This implies that the downward continuation makes gravity increase in average.

Summing the downward continuation of the Helmert gravity anomalies and the downward continuation of $2T^h/R$, we obtain the downward continuation of the Helmert gravity disturbances (Fig. 10). Note that since the downward continuation of $2T^h/R$ is rather small compared to the Helmert anomalies, the distribution of the Helmert gravity disturbances is almost the same in magnitude as that of the Helmert gravity anomalies. This can be understood from Eq. (16), remembering that the DT term is relatively small.

Finally, we summarize. This research dealt with some theoretical and numerical problems of the downward continuation of mean Helmert gravity disturbances. It shows that the downward continuation of $5' \times 5'$ mean Helmert gravity anomalies or disturbances may be undertaken to any desired accuracy without any difficulty. We proved that the contribution from the downward continuation of disturbing potential term is much smoother than that from the gravity anomaly disturbance and is two orders of magnitude smaller, so that it can be estimated from a global potential model. The numerical results showed that for calculating the trun-

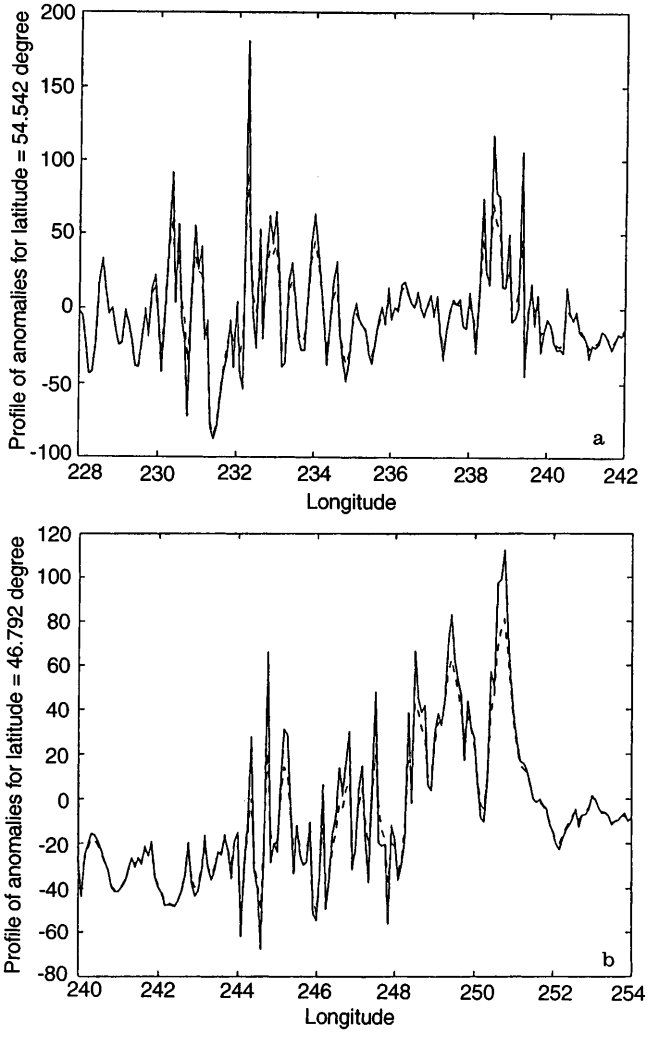

Fig. 9a, b. Comparison of the high-frequency part of the mean Helmert's gravity anomalies (mGal) on topography (*dashed line*) and on geoid (*solid line*) for **a** a profile at $\phi = 54°.542$, and **b** a profile at $\phi = 46°.792$

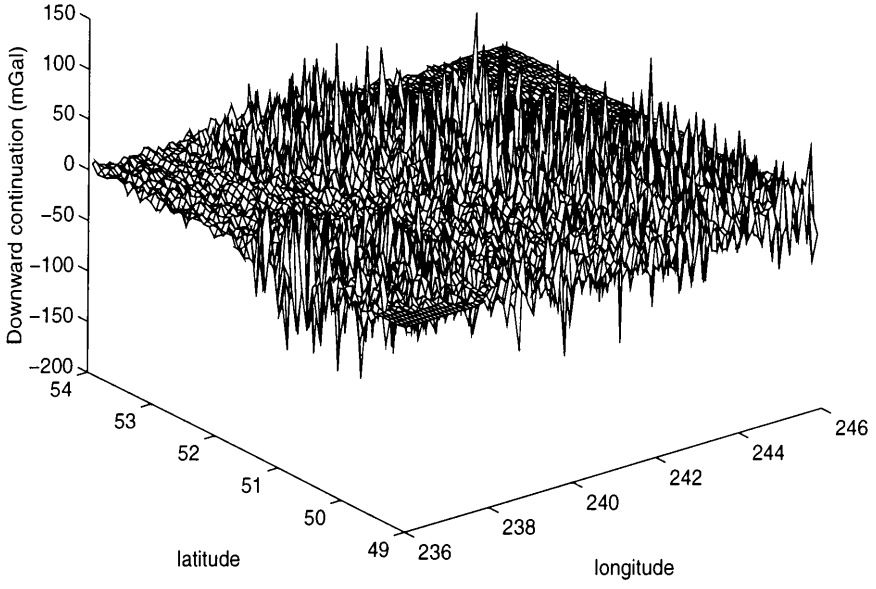

Fig. 10. Downward continuation of the high-frequency part of the $5' \times 5'$ mean Helmert gravity disturbances $(D\delta g^h)^L$ (mGal)

cation error of the truncated Poisson integral, the first 180° of a global potential model are sufficient. We discussed the convergence of the mean iterative scheme (Vaníček et al. 1996) for calculating the Poisson integral. We proved that the mean iterative scheme is convergent. The convergence speed depends on the topographical heights and at most 80 iterations are enough anywhere in Canada to reach an accuracy of 0.01 mGal in Tchebyshev norm. As a numerical integration, the mean iterative scheme gives a more reasonable and reliable solution than the point scheme.

Acknowledgements. We wish to acknowledge that Wenke Sun was supported by an NSERC International Fellowship grant and Petr Vaníček by an NSERC operating grant. We thank Mr. M. Véronneau of the Geodetic Survey Division for providing us with all the data used here. Thorough and helpful reviews of the manuscript by Dr. M. Vermeer and two anonymous reviewers are gratefully acknowledged.

References

Bjerhammar A (1963) A new theory of gravimetric geodesy. Royal Institute of Technology, Stockholm

Bjerhammar A (1964) A new theory of geodetic gravity. Royal Institute of Technology, Stockholm

Bjerhammar A (1987) Discrete physical geodesy. Rep. 380, Dept Geod Sci Surv. Ohio State University, Columbus

Gruber T, Anzenhofer M (1993) The GFZ 360 gravity field model, the European geoid determination. In: Eds. R. Forsberg and H. Denker (ed) Proceedings of session G3, European Geophysical Society XVIII General Assembly. KMS, Copenhagen

Heiskanen WH, Moritz H (1967) Physical geodesy. Freeman, San Francisco

Martinec Z (1996) Stability investigations of a discrete downward continuation problem for geoid determination. J Geod 70: 805–828.

Martinec Z, Vaníček P (1994) Direct topographical effect of Helmert's condensation for a spherical approximation of the geoid. Manuscr Geod 19: 257–268

Molodenskij MS, Eremeev VF, Yurkina MI (1962) Methods for study of the external gravitational field and figure of the earth. English translation by Israel Programme for Scientific Translations, Jerusalem, for Office of Technical Services, Dept Commerce, Washington, DC

Moritz H (1980) Advanced physical geodesy. Wichman, Karlsruhe

Vaníček P, Kleusberg A (1987) The Canadian geoid – Stokesian approach. Manuscr Geod 12: 86–98

Vaníček P, Krakiwsky EJ (1986) Geodesy: the concepts (2nd edn). North Holland, Amsterdam

Vaníček P, Martinec Z (1994) The Stokes-Helmert scheme for the evaluation of a precise geoid. Manuscr Geod 19: 119–128

Vaníček P, Sjöberg LE (1991) Reformulation of Stokes's theory for higher than second-degree reference field and a modification of integration kernels. J Geophys Res 96: 6529–6539

Vaníček P, Sun W, Ong P, Martinec Z, Vajda P, Horst B (1996) Downward continuation of Helmert's gravity. J Geod 71: 21–34

Wichiencharoen C (1982) The indirect effects on the computation of geoid undulations. Dept Geod Sci Rep 336. Ohio State University, Columbus